THE EFFECT OF EQUAL CHANNEL ANGULAR PRESSING ON THE PARTICLE DISTRIBUTION AND FRACTURE PROPERTIES OF A METAL MATRIX COMPOSITE

I. Sabirov[1], O. Kolednik[1], R. Z. Valiev[2], R. Pippan[1]

[1] Erich Schmid Institute of Materials Science, Austrian Academy of Sciences,
Jahnstrasse 12, Leoben, 8700, Austria
[2] Institute of Physics of Advanced Materials, Ufa State Aviation Technical University,
K. Marx street 12, Ufa, 450000, Russia

ABSTRACT

The effect of equal channel angular pressing (ECAP) on the homogeneity of the particle distribution and the fracture properties of an Al6061-20%Al_2O_3 composite processed by powder metallurgy (PM) technology is investigated. The as-fabricated material shows a strongly clustered particle distribution. The material is subjected to ECAP for 4 and 7 passes. For each condition, the homogeneity of the particle distribution in the matrix is studied by the quadrat method. Standard tensile and fracture mechanical tests are performed to determine the mechanical properties and the J-integral resistance curves of the material. It is shown that the application of ECAP significantly improves the homogeneity of the particle distribution and, as a result, the fracture properties.

1. INTRODUCTION

Metal matrix composites (MMCs) are increasingly used for automative and aerospace structures due to their improved mechanical properties [1, 2]. MMCs reinforced by small (less than 10 μm) particles would be especially interesting for industry, since such reinforcements lead to high mechanical properties [1]. However, these materials are prone to cause an inhomogeneous particle distribution [3]. As well known, a presence of particle clusters can significantly degrade the formability of MMCs due to localisation of plastic flow in particle clusters [4].

Secondary processing methods, such as extrusion or rolling, are used to improve the homogeneity of the particle distribution in MMCs [1, 3]. Tan and Zhang [3] proposed a model to predict the homogeneity of the particle distribution in an MMC processed by powder metallurgy (PM) technology. They suggest that a homogeneous particle distribution can be expected, if the average particle size is higher than a critical particle size, d_c, which is determined as

$$d_c = \frac{d_m}{\left[\left(\frac{\pi}{6f}\right)^{1/3} - 1\right]\sqrt{R}}. \quad (1)$$

d_m is the matrix powder size, f the particle volume fraction, and R the extrusion ratio. It follows from Eq. 1 that the extrusion ratio is for a given material the only parameter responsible for the homogeneity of the particle distribution in the PM-MMCs during its processing: an increase of the extrusion ratio leads to a decreasing d_c-value. According to this model, a homogeneous particle distribution can be achieved in any material, independently of the particle and matrix powder size or the particle volume fraction, if enough deformation is induced into the sample. However, a great shortcoming of extrusion is a significant decrease of the sample section with increasing extrusion ratio. Thus, the extrusion ratio is often limited by a fixed final dimension of the sample required for industrial application.

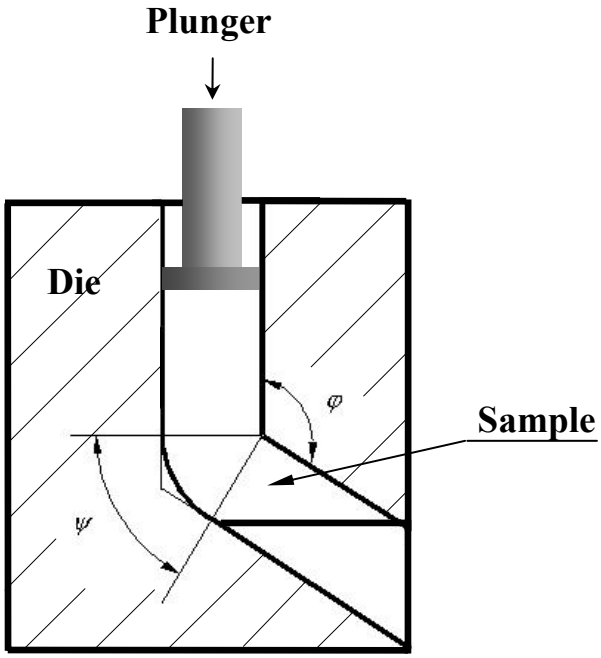

"**Fig. 1.** The principle of the equal channel angular pressing."

For this reason, a deformation method would be advantageous which induces intense strains into the sample without any change of the sample size.

The equal channel angular pressing (ECAP) might be an effective tool to solve this problem. In this method, intense plastic strains are induced into massive billets without changing their cross section [5, 6]. The ECAP facility consists of two channels which are equal in cross section (Fig. 1). The channels are intersected at a certain angle, φ. Another important parameter describing the ECAP facility is the angle subtended by the arc curvature, ψ. A sample is usually subjected to a multiple pressing through a die. An analysis performed in [6] has shown that the strains introduced into a sample during ECAP are a function of the angles φ and ψ, and the number of ECAP passes, N,

$$\varepsilon_{ECAP} = \frac{N}{\sqrt{3}}\left[2\cot\left(\frac{\varphi}{2}+\frac{\psi}{2}\right)+\psi\cdot\csc\left(\frac{\varphi}{2}+\frac{\psi}{2}\right)\right]. \tag{2}$$

The extrusion ratio, R, in Eq. (1) is considered as a measure of strain induced into the sample. Actually, it is equal to the ratio of the final length of the sample after extrusion, l_f, to its initial length, l_i. On the other hand, this ratio can be also presented as a function of the true strain induced into the sample by extrusion (Eq. 3) which follows from the general determination of the true strain, $\varepsilon = ln\,(l_f / l_i)$,

$$R = \exp(\varepsilon). \tag{3}$$

In the case of two step extrusion with extrusion ratios R_1 and R_2, a total extrusion ratio can be determined as $R = R_1 \cdot R_2$. So, if we combine extrusion and ECAP, a total extrusion ratio can be presented as

$$R = R_{ext} \cdot R_{ECAP}. \tag{4}$$

According to Eq. 3, R_{ECAP} can be determined as $R_{ECAP} = \exp(\varepsilon_{ECAP})$ or, taking into account Eq. 2, as

$$R_{ECAP} = \exp\left[\frac{N}{\sqrt{3}}\left[2\cot\left(\frac{\varphi}{2}+\frac{\psi}{2}\right)+\psi\cdot\csc\left(\frac{\varphi}{2}+\frac{\psi}{2}\right)\right]\right]. \quad (5)$$

Inserting Eq. 5 into Eq. 4, and obtained result into Eq. 1, we get an extension of the Tan and Zhang model for the case of combination of extrusion with ECAP:

$$d_c = \frac{d_m}{\left[\left(\frac{\pi}{6f}\right)^{1/3}-1\right]\sqrt{R_{ext}}\sqrt{\exp\left[\frac{N}{\sqrt{3}}\cdot\left[2\cot\left(\frac{\varphi}{2}+\frac{\psi}{2}\right)+\psi\cdot\csc\left(\frac{\varphi}{2}+\frac{\psi}{2}\right)\right]\right]}}. \quad (6)$$

Here, both the strains introduced during extrusion and ECAP are taken into account.

2. MATERIAL AND EXPERIMENTAL PROCEDURE

An Al6061 based PM-MMC reinforced by 20% of Al_2O_3 is chosen as the material for this investigation. The chemical composition of the matrix material is given in Table 1. The alumina particle size scatters in the range between 1 and 5 μm. A few, single particles having larger sizes are observed. The size of the matrix powder is 40 μm. The composite was supplied in form of a rod with a diameter of 25 mm; the extrusion ratio was 10:1. A metallographic section of the rod shows that the as-fabricated material has a strongly clustered particle distribution (Fig. 2a).

For the ECAP, the rod is cut into samples with a length of 100 mm. These samples are heated to 370°C and pressed repeatedly through the ECAP die. The parameters of the ECAP die are $\varphi = 90°$ and $\psi = 20°$ (Fig. 1). Between consecutive passes, the samples are rotated by 90°, always in the same direction. After 4 and 7 passes, the homogeneity of the particle distribution is studied.

For the microstructural investigation, the rods are sectioned in the longitudinal direction, grinded, polished, and investigated in the SEM.

For the analysis of the uniformity of particle distribution in the MMC, the quadrat method is used [7, 8]. In this method, the images are divided into a grid of square cells and the number of the particles in each cell, N_q, is counted. 9 micrographs from the center region of the specimens are taken in the SEM, each covering an area of 130×100 μm. Each image is divided into 140 quadrats. The size of each quadrat is set to $a = 8.5$ μm.

The histograms of the particle per quadrat distributions for each material condition are plotted. These histograms are compared with theoretical distributions: (1) the negative binomial distribution which corresponds to a perfectly clustered particle distribution; (2) the Poisson distribution corresponding to a homogeneous particle distribution [7, 8].

Specimens for mechanical tests were annealed at 530°C for 1h, quenched in water, and aged at 175°C for 15 min. which corresponds to an under-aged condition. This heat treatment was chosen because of the low fracture toughness of the MMC. It was shown in [9] that MMCs in the under-aged condition have the highest fracture toughness. In our case, a high fracture

"Table 1. The chemical composition of the Al6061 alloy."

Si	Fe	Cu	Mn	Mg	Zn	Cr	Ti
0.4÷0.8	0.7	0.15÷0.4	0.15	0.8÷1.2	0.25	0.04÷0.35	0.15

toughness would be advantageous to compare the fracture properties of the material.
Disk-shaped compact specimens with a thickness $B = 10$ mm, a width $W = 18.5$ mm, and a ratio of $a_0 / W \approx 0.5$ are used to perform the fracture tests. The specimens are pre-fatigued in compression and tension. The direct current potential drop technique is used to determine the crack propagation during the test. The J-Δa curves are determined according to the ASTM standard testing procedure [10].
Grinded and polished tensile specimens with a quadratic cross section of 2x2 mm and a gage length of 10 mm are used for the tensile tests.

3. RESULTS AND DISCUSSIONS

3.1. The effect of ECAP on the homogeneity of the particle distribution in the MMC

The critical particle size for each material condition calculated by Eq. 6 is given in Table 2. The d_c-value is equal to 33.4 μm for the as-fabricated condition. It is significantly higher than the average particle size of the MMC. As a result, a strongly clustered particle distribution is observed for this condition. The particle clusters are elongated in the extrusion direction: the clusters have a size of up to 40 μm in the direction perpendicular to the extrusion direction. Large particle free zones with a size of up to 200 μm in the extrusion direction and up to 40 μm in the transverse direction, are located between particle clusters (Fig. 2a). From Fig. 3a, it is seen that the histogram corresponding to the particle distribution for the as-fabricated material seems to follow the negative binomial distribution indicating a clustering.
After 4 ECAP passes, the d_c-value decreases significantly to 4.1 μm. This value corresponds to the upper boundary of the range of the reinforcement size in the MMC. Thus, the process of declustering should begin. Indeed, after 4 ECAP passes, the particle free zones become smaller and the particle clusters start to scatter (Fig. 2b). For this material condition, a deviation from the negative binomial distribution to the Poisson distribution can be noted in the histogram (Fig. 3b).
For the MMC after 7 ECAP passes, the d_c-value is equal to 0.9 μm. Since this value is less than the lowest bound of the particle size, complete particle declustering can be expected. Really, almost complete declustering and an absence of particle free zones are observed in Fig. 2c. The histogram of the particle distribution follows the Poisson distribution confirming the particle declustering, as well (Fig. 3c).
So, it can be concluded that the uniformity of the particle distribution increases with the numbers of ECAP passes. It is important to note that no particle breaking during the ECAP is observed. The mean values of the number of particles per quadrat, μ, are 6.2, 5.9, and 6.7 for the as-fabricated state, after 4 and 7 ECAP passes, respectively. It should be further noted that no voids are observed in the MMC after 7 ECAP passes.

3.2. The effect of ECAP on the mechanical properties of the MMC

The results of the tensile tests are given in Table 3. It is seen that the yield strength, σ_y, the ultimate tensile strength, σ_{UTS}, the strain hardening coefficient, N, and the fracture strain, ε_{fr},

"**Table 2.** Critical particle size for each investigated condition."

Number of ECAP passes	0	4	7
d_c [μm]	33.4	4.1	0.9

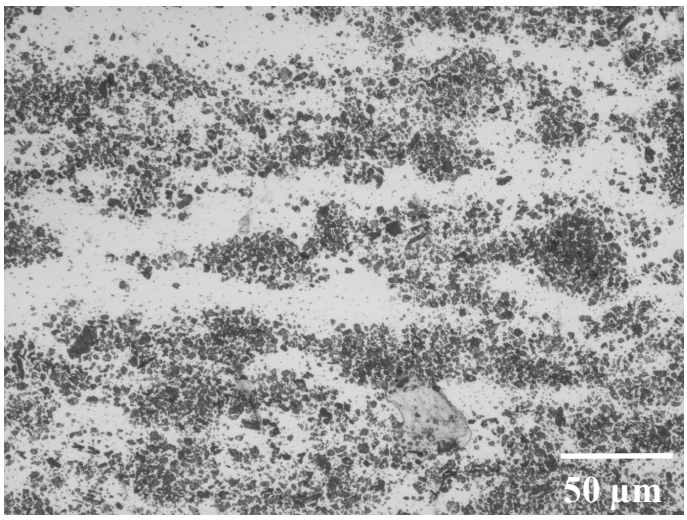

a)

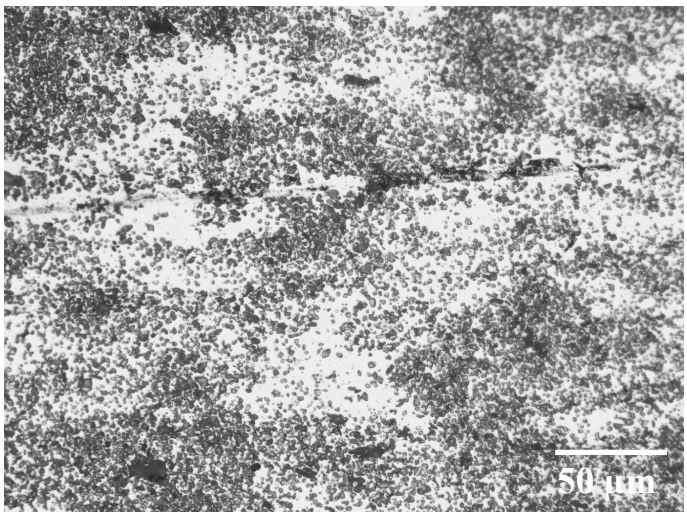

b)

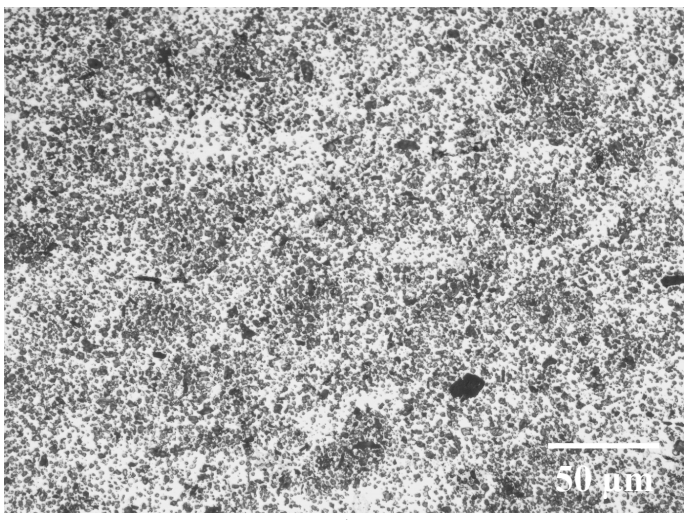

c)

"**Fig. 2.** The microstructure of the MMC: a) in the as-fabricated condition, b) after 4 ECAP passes, c) after 7 ECAP passes."

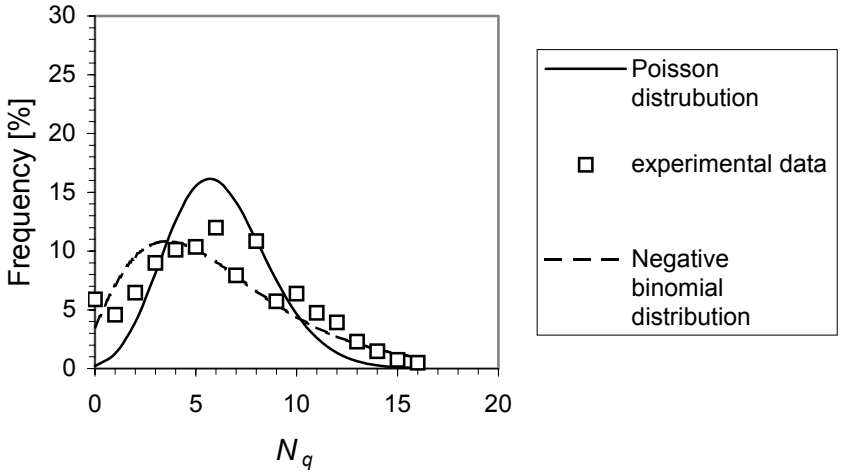

a)

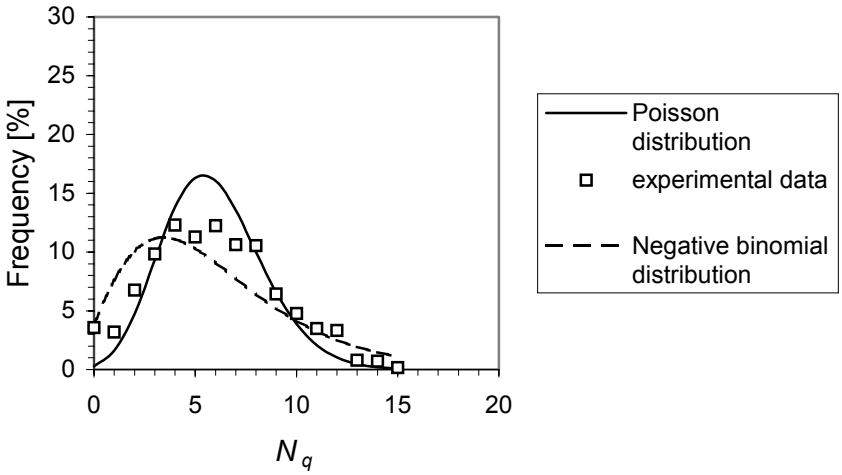

b)

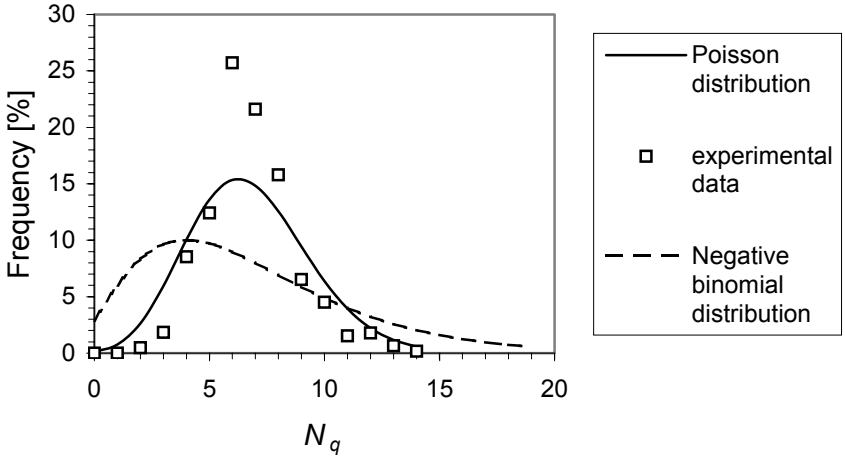

c)

"**Fig. 3.** Theoretical distribution curves and experimental results from the quadrat analysis of: the MMC: a) in the as-fabricated condition, b) after 4 ECAP passes, c) after 7 ECAP passes."

"**Table 3.** Data on mechanical properties of the MMC."

Number of ECAP passes	σ_y [MPa]	σ_u [MPa]	N	ε_{fr} [%]	$J_{0.2}$ [kN/m]	$dJ/d(\Delta a)$ [kN/m^2]	Δa_{stab} [mm]	R_{tot} [kJ/m^2]
0	225	287	0.11	3.0	1.5	1.93	0.42	7.7
4	230	315	0.12	4.2	1.7	2.50	0.72	10.3
7	230	306	0.12	3.5	2.7	3.88	1.05	15.4

do not change significantly with increasing uniformity of the particle distribution.
In Figure 4, the J-Δa curves for all disk-shaped compact specimens are given. The values of the fracture initiation toughness, $J_{0.2}$, the maximum extension of the stable crack propagation, Δa_{stab}, and the slope of the J-Δa curve, $dJ/d(\Delta a)$ (which was determined in the range between $\Delta a = 0.2$ mm and Δa_{stab}) are listed in Table 3, as well. In comparison with the tensile testing data, all these values increase significantly with increasing homogeneity of the particle distribution. For instance, the $J_{0.2}$-value of the MMC after 7 ECAP passes is by 80% higher than for the as-fabricated material.
The slope of the J-Δa curves, $dJ/d(\Delta a)$, is especially interesting, as this parameter is a measure of the total crack growth resistance of the material, R_{tot}, [11, 12]. In [11], the relation between the R_{tot} and the slope of the J-Δa curve was derived,

$$\frac{dJ}{d(\Delta a)} \approx \frac{\eta}{b} R_{tot}, \tag{7}$$

where η is the pre-factor in the J-evaluation formula [10], and b the ligament length $b = W$-a. The R_{tot}-values calculated by Eq. 7 are also listed in Table 3. A significant increase of the R_{tot}-values with increasing homogeneity of the particle distribution is observed: the R_{tot}-value of the MMC after 7 ECAP passes is higher than the R_{tot}-value of the as-fabricated MMC by a factor of 2. As was shown in [11], for the flat-fracture region, R_{tot} is determined by the plastic energy to form the fracture surface and the energy spent below the fracture surface.
A significant difference in the morphology of the fracture surfaces can be noted. A vast amount of particle clusters on the fracture surfaces is seen in the as-fabricated material (Fig. 5a). In Figure 5b, a region of a broken particle cluster is given at higher magnification. No matrix material is observed between the alumina particles in the cluster. Few regions consisting of dimples can be also observed. On the contrary, the fracture surface of the MMC after 7 ECAP passes looks more homogeneous (Fig. 5c). It consists mostly of dimples initiated by a particle/matrix decohesion mechanism. These dimples are shown in Fig. 5d at higher magnification. From the qualitative analysis of the fracture surfaces, it is clear that the plastic energy to form the fracture surface in the MMC after 7 ECAP passes is higher in comparison with this energy for the as-fabricated material, as no energy is required for void formation and their further growth in the particle clusters (Fig. 5b).
Currently, investigations of the local fracture toughness near the crack front at regions with particle clusters and in regions with a homogeneous particle distribution are undertaken.

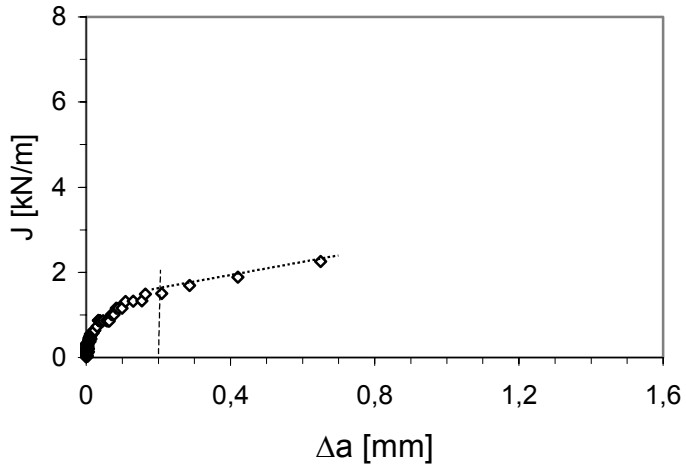

a)

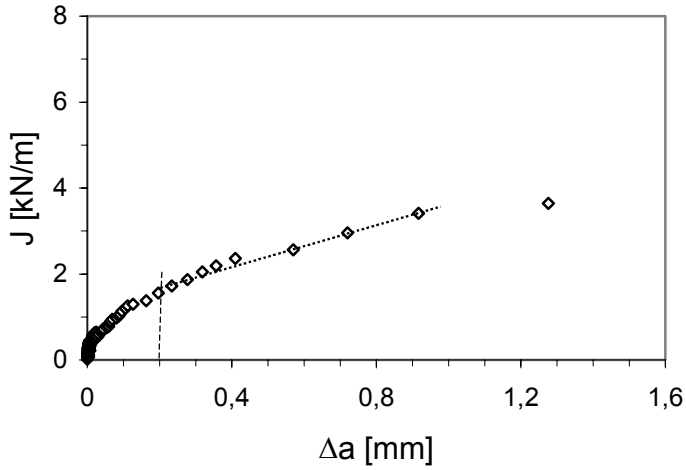

b)

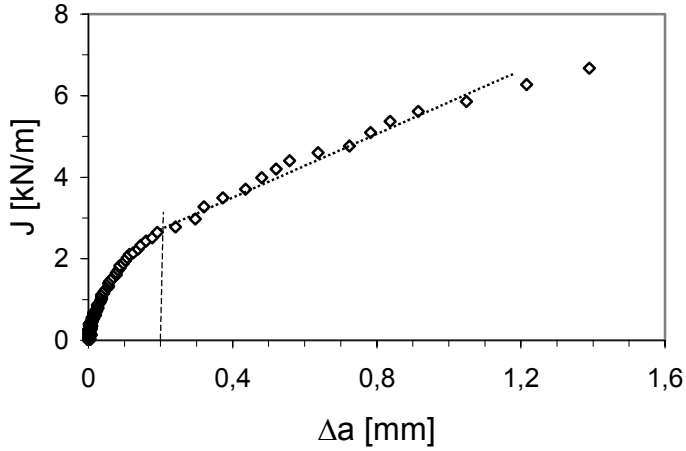

c)

"**Fig. 4.** The *J*-integral resistance curves for the MMC: a) in the as-fabricated condition; b) after 4 ECAP passes; c) after 7 ECAP passes."

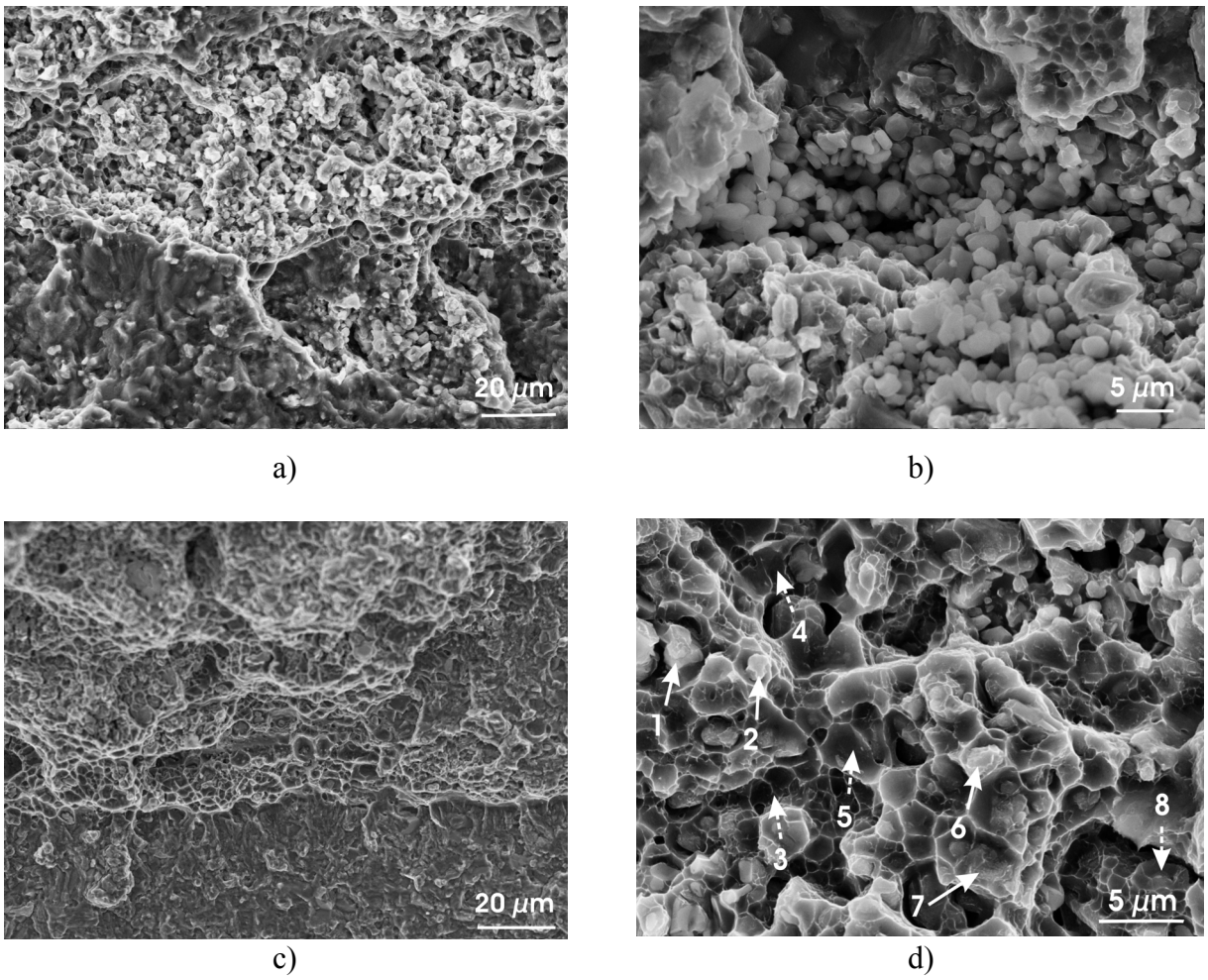

"**Fig. 5.** The fracture surface of the MMC: a, b) in the as-fabricated condition; c, d) after 7 ECAP passes."

4. CONCLUSIONS

1) An Al6061-20%Al_2O_3 metal matrix composite (MMC) processed by the powder metallurgy (PM) technology with strongly clustered particle distribution is subjected to equal-channel angular pressing (ECAP) at $T = 370°C$ for 4 and 7 passes. The effect of ECAP on the homogeneity of the particle distribution in the PM-MMC and its fracture properties is studied.
2) The model by Tan and Zhang [3] about the estimation of the critical value of the particle size which is required for a homogeneous particle distribution in the matrix is extended to the case of combination of extrusion and ECAP. It is shown that ECAP leads to a significant increase of the uniformity of the particle distribution. This is also shown by an analysis with the quadrat method which shows a transition from a negative binomial distribution (for the as-fabricated MMC) to the Poisson distribution (for the MMC after 7 ECAP passes).
3) No essential effect of the ECAP on the tensile testing data is found, whereas the fracture initiation toughness, $J_{0.2}$, the slope of the J-Δa curve, $dJ/d(\Delta a)$, and the total crack growth resistance, R_{tot}, significantly increase with increasing homogeneity of the particle distribution.

ACKNOWLEDGEMENTS
Authors acknowledge gratefully the financial support of this work by the Austrian Fonds zur Förderung der wissenschaftlichen Forschung under the project number P14333-PHY.

References

[1] **Clyne, T.V., Withers, P.J.**, "An Introduction to Metal Matrix Composites", Cambridge University Press, UK, 1993.
[2] **Kaczmar, J.W., Pietrzak, K., Wlosinski, W.**, "The production and application of metal matrix composite materials", J. Mater. Process Tech., 206 (2000), 58-67.
[3] **Tan, M.J., Zhang, X.**, "Powder metal matrix composites: selection and processing", Mater. Sci. Eng., A244 (1998), 80-85.
[4] **Prangnell, P.B., Barnes, S.J., Roberts, S.M., Withers, P.J.**, "The effect of particle distribution on damage formation in particulate reinforced metal matrix composites deformed in compression", Mater. Sci. Eng., A220 (1996), 41-56.
[5] **Valiev, R.Z., Islamgaliev, R.K., Alexandrov, I.V.**, "Bulk nanostructured materials from severe plastic deformation", Prog. Mater. Sci., 45 (2000), 103-189.
[6] **Iwahashi, Y., Wang, J., Horita, Z., Nemoto, M., Langdon, T.G.**, "Principle of equal-channel angular pressing for the processing of ultra-fine grained materials", Scripta Mater., 35 (1996), 143-146.
[7] **Rogers, A.**, "Statistical Analysis of Spatial Dispersions: The Quadrat Method", Pion, London, UK, 1974.
[8] **Karnezis, P.A., Durrant, G., Cantor, B.**, "Characterisation of reinforcement distribution in cast Al-alloy/SiC_p composites", Mater. Charact., 40 (1998), 97-109.
[9] **Pandey, A.B., Majumdar, B.S., Miracle, D.B.**, "Deformation and fracture of a particle-reinforced aluminum alloy composites: Experiments", Metal. Mater. Trans., 31 (2000), 921-936.
[10] **ASTM E1820-01**, "Standard Test Method for Measurement of Fracture Toughness", Annual Book of Standards, American Society of Testing and Materials, Philadelphia, USA, 2001.
[11] **Stampfl, J., Kolednik, O.**, "The separation of the fracture energy in metallic materials", Int. J. Fracture, 101 (2000), 321-345.
[12] **Kolednik, O.**, "On the physical meaning of the J-Δa-curves", Eng. Fract. Mech., 38 (1991), 403-412.